Journal of the Mechanical Behavior of Biomedical Materials 76 (2017) 97–103

Contents lists available at ScienceDirect

Journal of the Mechanical Behavior of Biomedical Materials

journal homepage: www.elsevier.com/locate/jmbbm

The nonlinear flexural response of a whole teleost fish: Contribution of scales and skin

Lawrence Szewciw[a], Deju Zhu[a,b], Francois Barthelat[a,*]

[a] Department of Mechanical Engineering, McGill University, Macdonald Engineering Building, 817 Sherbrooke St. West, Montreal, Quebec, Canada H3A 0C3
[b] College of Civil Engineering, Hunan University, Changsha, Hunan Province 410082, China

ARTICLE INFO

Keywords:
Teleost fish
Flexural stiffness
Fish scale
Tendon effect
Locomotion

ABSTRACT

The scaled skin of fish is an intricate system that provides mechanical protection against hard and sharp puncture, while maintaining the high flexural compliance required for unhindered locomotion. This unusual combination of local hardness and global compliance makes fish skin an interesting model for bioinspired protective systems. In this work we investigate the flexural response of whole teleost fish, and how scales may affect global flexural stiffness. A bending moment is imposed on the entire body of a striped bass (*Morone saxatilis*). Imaging is used to measure local curvature, to generate moment-curvature curves as function of position along the entire axis of the fish. We find that the flexural stiffness is the highest in the thick middle portion of the fish, and lowest in the caudal and rostral ends. The flexural response is nonlinear, with an initial soft response followed by significant stiffening at larger flexural deformations. Low flexural stiffness at low curvatures promotes efficient swimming, while higher stiffness at high curvatures enables a possible tendon effect, where the mechanical energy at the end of a stroke is stored in the form of strain energy in the fish skin. To assess the contribution of the scales to stiffening we performed flexural tests with and without scales, following a careful protocol to take in account tissue degradation and the effects of temperature. Our findings suggest that scales do not substantially increase the whole body flexural stiffness of teleost fish over ranges of deformations which are typical of swimming and maneuvering. Teleost scales are thin and relatively flexible, so they can accommodate large flexural deformations. This finding is in contrast to the bulkier ganoid scales which were shown in previous reports to have a profound impact of global flexural deformations and swimming in fish like gar or *Polypterus*.

1. Introduction

The scaled skin of fish is a natural material that has received examination recently as a source of inspiration for the fabrication of biomimetic protective systems (Martini et al., 2017; Martini and Barthelat, 2016a; Ghosh et al., 2014; Browning et al., 2013; Rudykh et al., 2015). Research on the mechanical properties of fish skin has focused on elucidating the specialized mechanisms underlying the enhanced protective properties of this biological material against predators and other mechanical disturbances (Bruet et al., 2008; Meyers et al., 2012; Zhu et al., 2012; Yang et al., 2013; Zhu et al., 2013). In particular, the high contrast of stiffness between the scale and the surrounding tissues gives rise to unusual and attractive mechanisms related to flexibility (Ghosh et al., 2014; Martini and Barthelat, 2016a) and resistance to fracture (Chintapalli et al., 2014) or tilting (Martini and Barthelat, 2016b). The scaled skin of teleost fish has evolved high protective capacity in combination with several other properties that would be considered desirable in protective systems or body armor, for example it is thin, flexible, light weight, transparent and breathable (Zhu et al., 2013; Elliot, 2000). Characterization of the structural and mechanical properties of fish skin in order to explain and replicate its optimized protective function commenced with study of individual dermal scales, ranging from histological evaluation and mechanical testing (Zhu et al., 2012; Ikoma et al., 2003; Torres et al., 2008; Garrano et al., 2012) to measurement of penetration resistance and puncture mechanisms (Bruet et al., 2008; Meyers et al., 2012; Zhu et al., 2012). At the tissue level, teleost fish skin is composed of several overlapping scales arranged in precise, species-specific squamation patterns (Elliot, 2000), and additional mechanisms of scale interaction may further synergize puncture resistance of fish skin at higher length scales.

In a more recent study, Zhu et al. (2013) investigated key mechanisms and parameters controlling the high puncture resistance of teleost fish skin, and demonstrated that the scales mechanically interact and redistribute the force upon puncture over large volume and thus

* Corresponding author.
E-mail addresses: lawrence.szewciw@mail.mcgill.ca (L. Szewciw), dzhu@hnu.edu.cn (D. Zhu), francois.barthelat@mcgill.ca (F. Barthelat).

http://dx.doi.org/10.1016/j.jmbbm.2017.06.014
Received 10 April 2017; Received in revised form 8 June 2017; Accepted 10 June 2017
Available online 13 June 2017
1751-6161/

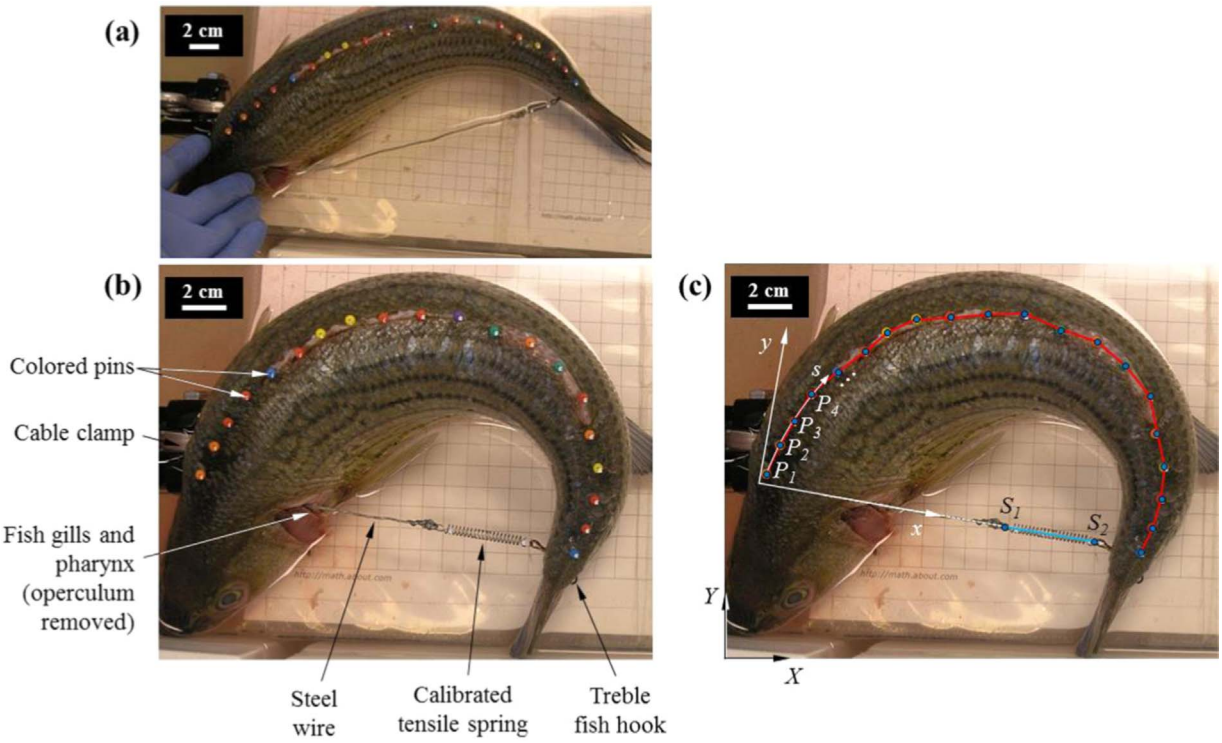

Fig. 1. (a) Initial near-straight bending position of fish used in flexural tests (zero force in spring). (b) Experimental setup for flexural tests on whole fish (shown at the maximum bending position). (c) Location of key points $P_1 \ldots P_N$ (digitized pin coordinates), S_1 and S_2 (spring coordinates) from image analysis. Global (X-Y), local (x,y) and curvilinear (s) coordinates are used.

limit local deflection and prevent damage to the soft underlying tissue. This finding was the first experimental data in support of the model of fish scale interaction upon puncture proposed by Vernerey and Barthelat (2010). However, as described in Vernerey and Barthelat (2010), this model of scale interaction may apply not only to puncture events, but also to whole fish bending during locomotion where progressive interlocking of scales may play a role in the undulatory locomotion of teleost fish. That is, fish scales on the inner, concave side of a bent teleost during swimming could potentially mechanically interact to assist with locomotion by increasing whole fish flexural stiffness at high body curvatures at the end of a swimming stroke, thus providing an exotendon (energy storage/release) effect and facilitating muscle contraction of the next swimming stroke. In this scenario, the scales deform and accumulate elastic strain energy at the end of each stroke, which can be recovered to initiate and rapidly accelerate the next stroke. The scales would therefore function as an external tendon (or exotendon) to enhance swimming efficiency (reduce the energy required for locomotion). The exotendon hypothesis was originally proposed by Wainwright et al. (1978) for the underlying dermal stratum (s.) compactum layer of skin (a cross-helical arrangement of collagen fibres) on the stretched convex side of the bent fish during locomotion, and using skin from the lemon shark, *Negaprion brevirostris*. The possible exotendon function of the s. compactum was further explored by Hebrank and Hebrank (1986) for two species of teleost fish: Norfolk spot, *Leiostomus xanthurus*, and skipjack tuna, *Katsuwonus pelamis*, and by Naresh et al. (1997) for the spadenose shark, *Carcharias laticaudus*. The potential role of scaled fish skin in increasing whole fish flexural stiffness at high body curvatures was first investigated by Long et al. (1996) using a ganoid fish (longnose gar, *Lepisosteus osseus*). These researchers determined a significant decrease in whole fish flexural stiffness after incision of the dermis and removal of a single row of scales at a caudal location on the fish. However, Long et al. (1996) only focused on ganoid fish, and did not describe a potential whole body exotendon effect. Here, we explore potential exotendon effects in the teleost fish striped bass, *Morone saxatilis*, which are covered with "lighter" scales compared to gar. In particular, we assess the potential contribution of the scales in this mechanism through flexural tests on the whole body of the fish.

2. Material and methods

2.1. Sample collection and dissection

Whole, fresh (recently deceased and on ice) striped bass (*Morone saxatilis*) fish ($N = 3$), a common teleost from the northern Atlantic Ocean, were acquired from a local fish store (Montreal, QC, Canada). The fish originated from the fish supplier, Nature's Catch Inc., Clarksdale, MS, USA. The fish had a total length (l) and width (w) of about (~) 40 cm and 10 cm, respectively, and were kept on ice before testing. All tests were commenced within a few hours of purchasing the fish specimens and the fish were preconditioned once before tests by rinsing with cold tap water and gently flexing the fish for about five minutes, in order to raise the temperature of the fish samples and bring them closer to physiological body conditions (the flexural rigidity of the samples was notably lower after preconditioning). The fish samples were briefly dissected before being half-submerged in ice water for the duration of tests (as described below), to maintain the samples at the same temperature and hydration conditions that were similar to the natural environment of striped bass, which survive in a wide range of environmental conditions including water temperature (Hodson, 1989). With reference to De luliis and Pulera (2001), the anterior and posterior dorsal fins and the caudal fin of the fish were removed using large dissecting scissors to clearly expose the mid-dorsal line of the fish and allow for insertion of push pins. The caudal fin of the fish was removed to allow for a full range of motion of the fish during bending tests using the experimental setup. In order to track the position of the spine, about 20 push pins were inserted into the body of the fish along the mid-dorsal line from the tail region to the start of the cranium and spaced ~12.5 mm apart (Fig. 1a). The pins were small and short enough that they did not disrupt the whole structure of the fish, and the impact on

flexural behavior was insignificant since the pins were attached on the flexural "neutral plane" where there is no stress/strain when bending is imposed. In order to allow head-to-tail attachment of the fish with a cable and spring to measure forces upon flexure (as described below), a hole was then perforated through the thickness of the body in the tail region below the last pin and in the dorso-ventral midline. The opercular bones on the pharyngeal region on both sides of the fish were removed to expose the gills and pharynx, and a small passage was cleared through the thickness of the rostrum via the pharyngeal cavity. Removal of the operculum and the small passage through the rostrum may have slightly reduced the local flexural stiffness of the anterior region of the fish. However, at the point of attachment the bending moment generated by the spring is zero, and therefore no flexural deformation is expected. The effect of the dissection on the measured properties was therefore minimal and did not affect comparison of natural and descaled conditions.

The fish was placed belly down on an immersible support board, which consisted of a Plexiglas board covered with cm graph paper and plastic sheet, with a clamp fixed to one end of the board. The entire support board including the fish was submerged into a cooler of ice water and leveled so that the ventral half of the fish was underwater. Head-to-tail attachment first included inserting a treble fish hook through the hole in the tail so that the three points of the hook were securely embedded in the right side of the tail and the eye of the hook protruded through the left side of the tail. A precision extension spring was attached at one end to the eye of the treble hook, and braided steel wire was tied to the other end of the spring. The steel wire was then carefully fed through the fish's pharyngeal cavity from the left to right side of the rostrum, and connected to the clamp in a rope and pulley manner. The length of the head-to-tail attachment could then be adjusted by sliding the wire through the pharyngeal cavity, thereby inducing bending onto the body of the fish. The clamp on the convex side of the head was used to secure the wire and set the bending to a desired position. The spring was selected carefully so that it provided enough stiffness to enable large fish bending while it was soft enough to enable sufficient extensions for accurate force measurements from image analysis. Prior to the test, the force-extension response of the spring was calibrated by attaching a series of weights and taking pictures and a stiffness $k = 0.623$ N/mm was measured. An Olympus digital camera (model no. C-5060) on a tripod was positioned over the cooler in order to take high-resolution images of the entire fish at each bending position for image analysis.

2.2. Testing procedure

Bending tests commenced with the fish in a near-straight body position and the wire slack. The wire was then pulled and the fish was bent until the wire was taut, and a first image was acquired. The wire was then pulled by small (~1 N) increments, and a picture was taken at each bending position until a high body curvature was achieved. About fifteen bending positions were recorded per test, the maximum bending position (Fig. 1b,c) being significantly larger than the amplitude during normal swimming and approached bending that occurs during sharp turns or escape responses (Jayne and Lauder, 1995), and thus the results may only apply to rapid swimming or startle responses in this species. From the images in Fig. 1b,c, the fish is clearly in a state of high body curvature, which would be expected to be greater than the curvature observed from natural body undulations during the carangiform style of undulatory locomotion exhibited by this teleost fish (Jayne and Lauder, 1995). The fifteen bending positions for each flexural test therefore ranged from a near-straight body configuration (with no flexural resistance), to the end of the "neutral zone" (Long et al., 1996) or region of low flexural stiffness at low body curvatures, and were completed at a high degree of body curvature that approximated the level of bending that occurs during sharp turns or escape responses (and possibly rapid swimming) (Jayne and Lauder, 1995). The test was performed two additional times on the same fish in order to verify repeatability. Upon completion of the first three scaled (natural, intact) tests, the fish was entirely descaled by gently plucking the scales using tweezers. The fish was descaled across both lateral body surfaces from the head to the tail fin, up to the dorsum and across the whole ventrum. The fish was replaced atop the support board and in the cooler for another three tests in the descaled state. Finally, using a 500 μm control-depth surgical knife, nine vertical incisions were made to the skin on both sides of the fish from the anterior to the posterior region (incision length ~32 mm, anteroposterior spacing ~25 mm). The 500 μm control-depth knife allowed precise disruption of the s. compactum layer of the skin without significant damage to the underlying muscle, because our histology results suggested that the hypodermis, the intervening tissue layer between the s. compactum and underlying muscle, is on average located at a depth of ~500 μm from the skin surface. The fish samples with disrupted s. compactum were tested three times. The onset and duration of rigor mortis is known to vary between species of teleost fish (from several hours to a few days), and is affected by factors such as temperature, handling, size and physical condition of the fish (Huss, 1995). The fish samples were likely post-rigor mortis and some tissue degradation may have occurred before sample collection (Huss, 1995). Therefore, the flexural properties of the fish and effects of descaling were possibly somewhat different than those of living fish with active and stiffer musculature, but as described in the results and discussion, the effect of descaling is likely similar. Also, comparing the percentage difference in flexural stiffness before and after descaling is a form of normalization that takes into account variation of absolute stiffness between the samples, including different level of "freshness" or even any differences in mechanical properties between live and dead tissue (post-rigor mortis). In order to test for possible degradation of properties during the course of flexural tests, another "control fish" was tested in bending at the very beginning of the test session, and subjected to the same temperature and hydration as the tested fish. The control fish was tested again at the very end of the session. No change in properties was observed in the control fish, and therefore no significant degradation of properties occurred over the course of the testing session.

2.3. Image analysis (coordinate selection)

For each picture, image analysis was used to locate the position of the pins (points P_1, P_2 … P_N), as well as the points S_1 and S_2 located at the ends of the spring. These coordinates were first determined in the global coordinate system (X,Y) (Fig. 1b). The points were digitized at high magnification (with single pixel resolution) using the software Plot Digitizer version 1.9 and converted to mm using the graph paper as reference. These coordinates were then processed using the software Matlab version R2011b. The coordinates of the points were first transformed into the (x,y) coordinate system, with the x axis aligned with the spring and the origin corresponding to the intersection between the axis of the spring and the mid-dorsal line on the fish's head (Fig. 1b). The procedure was repeated for each image, producing a series of fish profiles in the (x,y) coordinate system (Fig. 2). The curvilinear coordinate s of each pin was also computed from the x and y coordinates.

2.4. Data analysis

In the framework associated with (x,y) the head of the fish is fixed, and bending is induced by displacing the tail region along the x axis in the negative direction. The curvature of the fish was then determined as a function of the curvilinear coordinate s, by fitting an arc of a circle onto a Δs (seven data point) long segment of the profile centered on the point where curvature is to be determined. The curvature (mm^{-1}) was then simply determined by computing the inverse of the radius of the circle. Fig. 3a shows the local curvature of the fish as a function of

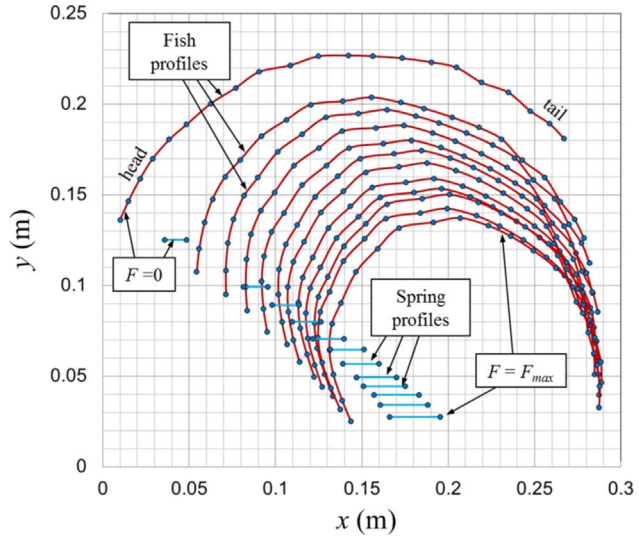

Fig. 2. Fish and spring profiles in the (x,y) coordinate system. Each data point corresponds to a digitized pin coordinate (P_1-P_{20}) with the axis of the spring (blue lines) aligned with the x axis and the origin set as the intersection between the line of force and the mid-dorsal line on the fish's head. Fish profiles for increasing force increments are shown from left (zero force) to right (maximum force).

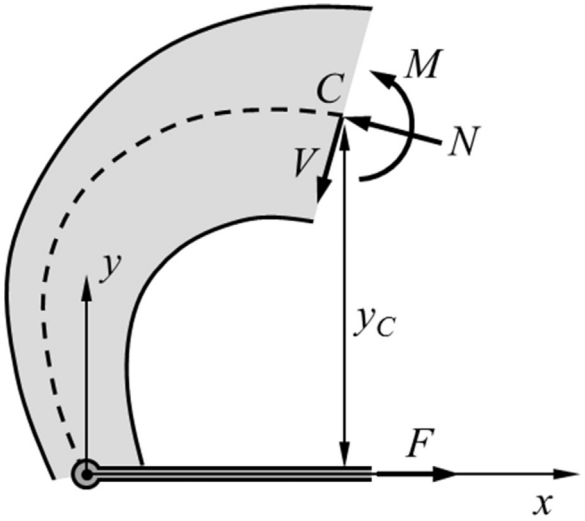

Fig. 4. Free body diagram of a section of the bent fish showing internal loads at point C: shear force (V), bending moment (M) and normal force (N). The tensile force in the cable is F. An important distance is y_C, the distance from the x axis to point C. The bending moment is zero at the head and tail attachment points.

position along the fish (curvilinear coordinate s) from one of the tests and as computed from the profiles of Fig. 2. The curvature is the highest near the tail, as suggested by the pictures shown in Fig. 1. Flexural properties cannot be inferred directly from this data, since the bending moment is also a function of curvilinear position, as explored below.

The coordinates of the points S_1 and S_2 were used to compute the extension of the spring, which was in turn used to calculate the tensile force via the calibrated spring constant. A convenient way to reveal the internal forces and moments in the system is to consider the free body diagram of the system "cut" along the fish at point C, and along the tensile line (Fig. 4). This "virtual cut" on the fish was taken along a cross section perpendicular to the mid-dorsal line of the fish (in the transverse plane), but not necessarily perpendicular to the spring. The application of a force F along the axis of the spring must be balanced by internal loads within the fish, exposed by the virtual cut at point C. Following conventions used for the bending of beams, these internal loads are represented as a normal force N, a shear force V and a bending moment M (Fig. 4). For the rest of the analysis we assumed that the normal and shear forces induce negligible deformations compared to the bending generated by the moment M. Only the moment M is then considered and its magnitude is simply given by $M = Fy_C$, where y_C is the vertical coordinate of point C (Fig. 4). Evidently the bending moment must be zero at the head and tail attachment points. Fig. 3b shows the local bending moment as a function of curvilinear position along the fish. For a fixed bending position and force in the spring, the middle

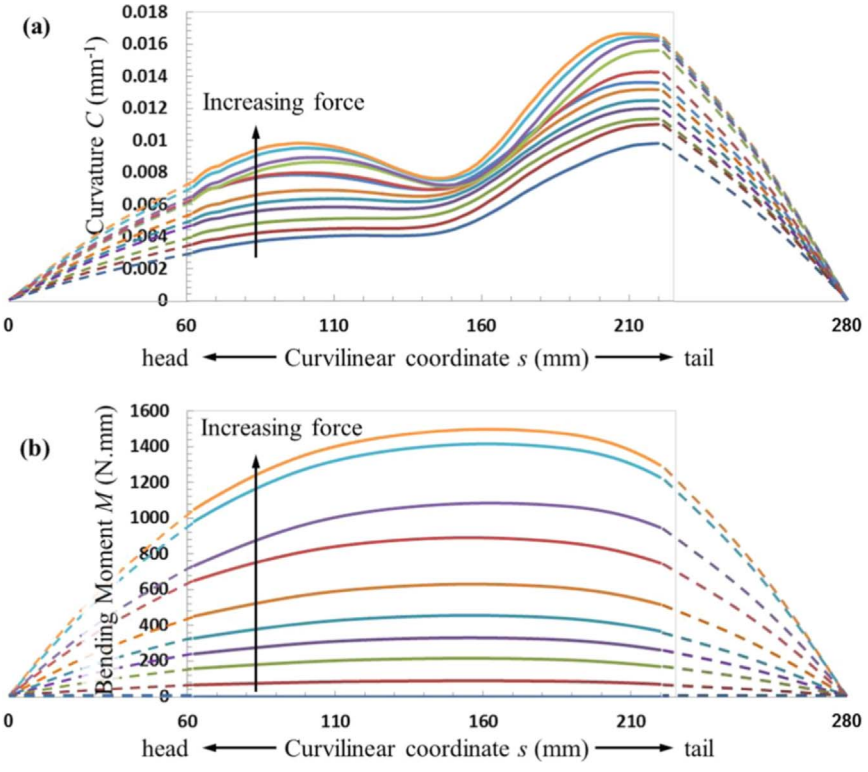

Fig. 3. (a) Local curvature C of the fish as a function of curvilinear coordinate s along the spine (b) Local bending moment M of the fish as a function of curvilinear coordinate s. Arrows labeled "increasing force" indicate the fish being flexed from the initial bending position (bottom curve) to the maximum bending position (top curve) during a single bending test. Dashed lines were extrapolated to the x axis where M and C are zero at the head and tail attachment points.

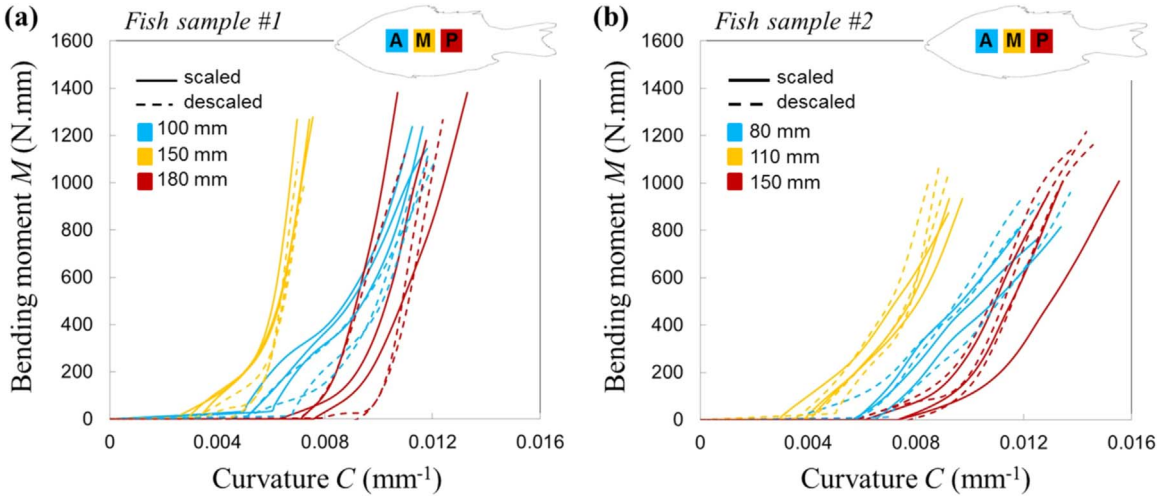

Fig. 5. Bending moment versus curvature at three locations along the anteroposterior axis of the fish: anterior (0–100 mm), mid (100–150 mm), and posterior (150–250 mm). (a) *M-C* curves at three locations along the mid-dorsal line of fish sample #1: at 100 mm in the anterior region, at 150 mm in the mid region, and at 180 mm in the posterior region. (b) *M-C* curves at 80 mm, 110 mm and 150 mm for fish sample #2.

region is subjected to the highest bending moment because it is the furthest from the line of action of the spring (i.e. *x* axis). As the bending increases, the bending moment at any point along the fish increases because both the tensile force in the spring and the distance from the line of action increase.

3. Results

3.1. Bending moment versus curvature at three locations (scaled vs. descaled)

This analysis produced a rich set of data for each test, where the curvature (C, mm^{-1}) and bending moment (M, N·mm) are known at any point along the mid-dorsal line of the fish. The fish was divided into three anteroposterior regions (curvilinear distances, s) along the mid-dorsal line: anterior (0–100 mm), middle (100–150 mm), and posterior (150–250 mm). Fig. 5 shows *M-C* curves as measured at three locations (curvilinear coordinates, s) along the mid-dorsal line: at 100 mm in the rostral region, at 150 mm in the trunk region, and at 180 mm in the caudal region for fish sample #1 (Fig. 5a), and at 80 mm, 110 mm and 150 mm for fish sample #2 (Fig. 5b). A similar shape was observed for *M-C* curves from all three regions of the fish. For low curvatures, the fish is highly flexible and requires negligible force to bend. At higher curvatures, significant stiffening is observed, up to a maximum curvature.

A clear softening or shifting of the *M-C* curves was not observed upon descaling of the fish, the scaled and descaled fish displaying similar results. This was evident from the similar shape and typical overlap in the range of natural and descaled curves in terms of slope or stiffness and curvature at stiffening at any location on the fish. Any potential decrease in flexural stiffness after descaling of the fish is small or negligible and was not detected with this experimental setup. Using a moving average along the slope of the *M-C* curve, the percentage differences in mean maximum tangent flexural stiffness between the scaled versus descaled trials (3 trials each) were −11.2, +0.595 and +1.96% for fish #1 and +28.0, +61.8 and +17.7% for fish #2 at the anterior, mid and posterior body locations, respectively. Whereas fish #1 demonstrated almost no change in flexural stiffness at two of the three body regions and a small decrease in one region, fish #2 in fact exhibited increases in flexural stiffness at all three locations and particularly at the mid location, which further suggests an absence of a stiffening effect provided by the scales during flexure. Although similar results were observed for several fish during preliminary tests, data were thoroughly analyzed and reported for only two fish samples without statistics performed due to the observed minimal effect of descaling on fish flexural stiffness, the extensiveness of the data analysis, and the biomimetic aims of this research in revealing major effects on fish biomechanics and locomotion. The main objective of this study was to reveal a possible substantial decrease in stiffness or slope of the *M-C* curve upon descaling of the fish and not to determine precise mechanical properties of the fish in the natural or descaled condition, and these data demonstrated a lack of a major effect of descaling on the flexural response of the whole fish.

3.2. Bending moment versus curvature versus curvilinear distance

Comparison of *M-C* curves along the entire curvilinear length of the fish revealed a trend in the data. Although curves of similar shape were observed at different points along the mid-dorsal line of the fish, the curvature at (initial) stiffening and the stiffness varied with position. Fig. 6 shows a more comprehensive representation of the flexural behavior of the whole fish, consisting of a surface in the (s,C,M) space. This 3D plot of M versus C along the entire curvilinear length of the fish reveals an obvious pattern in the *M-C* curves in that lowest curvature at stiffening and highest stiffness occurs near the middle or trunk portion of the fish centered at a curvilinear distance of ~150 mm (with minor variation between fish samples in stiffness at any body location and in the precise location of maximal stiffness in the trunk region). This region of higher stiffness manifests as a distinct ridge on the surface plotted in 3D space, the ridge tapering off in both anterior and posterior directions towards the softer head and tail regions.

3.3. Bending moment versus curvature at three locations (descaled vs. incised)

Fig. 7a shows the pattern of incisions prepared on the s. compactum of a descaled fish, and Fig. 7b shows *M-C* curves measured at three locations along the mid-dorsal line: 100 mm in the anterior region, 140 mm in the mid-region, and at 180 mm in the posterior region. A rightward shift of the *M-C* curves and decrease in flexural stiffness along the *M-C* curve was observed at all three anteroposterior locations upon s. compactum incision (Fig. 7b). The percentage differences in mean maximum tangent flexural stiffness between the descaled versus incised trials (3 trials each) were −25.6, −73.0 and −82.5% at the anterior, mid and posterior body locations, respectively. The fish therefore exhibited notable decreases in flexural stiffness at all three locations, and this decrease was the most pronounced at the posterior location. These results suggest that the s. compactum carries a

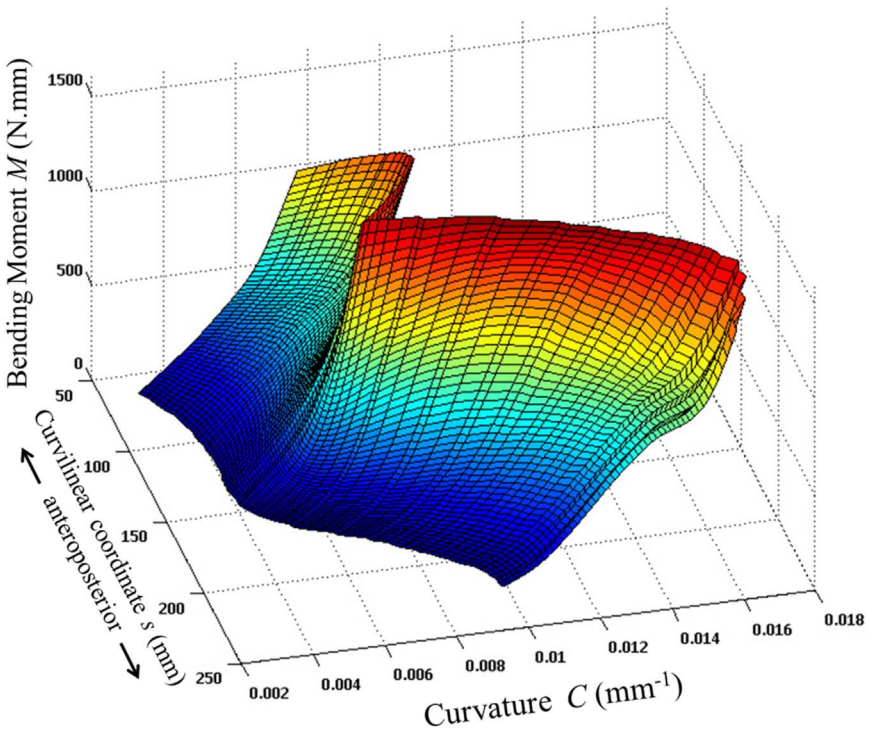

Fig. 6. Surface plot of bending moment-curvature at positions along the entire curvilinear length (*s*) of the fish in the natural condition (i.e. with scales), from a single flexural test.

significant portion of the bending moment. From previous work and observations this variation may be due to (i) stiffer s.compactum in these regions and/or (ii) morphological and structural variations along the length of the fish. In a recent article (Szewciw and Barthelat, 2017), we reported variations in structure and tensile properties of the s. compactum along the anteroposterior length of the fish. In particular, we found that the s. compactum in the posterior region was significantly stiffer than at other locations on the skin, which could explain its greater role in overall stiffness. In addition, since the rostral and caudal ends of the fish are notably thinner than the middle portion, it is possible that the s. compactum (which has relatively constant thickness of about 500 μm) accounts for a larger proportion of the flexural stiffness of the fish in the head and tail regions, and also suggests possible differences in external tendon function of the s. compactum along the length of the fish.

4. Discussion

The nonlinear flexural behavior of striped bass observed in this study is similar to the results reported by Long et al. (1996) on longnose gar, *L. osseus*. The *M-C* curves produced by Long et al. (1996) for gar fish exhibit the same general shape as we observed for striped bass, *M. saxatilis*. However, whereas maximal curvature is similar for both fish types (16 m^{-1} for the tail region of striped bass and 35 m^{-1} for gar), the maximal bending moment measured by Long et al., (1996) (~0.04 N.m) is 35 times lower than observed for striped bass (~1.4 N.m). This is likely due to the similar length, but substantially lower diameter of longnose gar compared to striped bass. Similar effects of body size and cross-sectional shape on body flexibility were demonstrated by Aleyev (1977), and described by Tytell et al. (2010), using a variety of fish species ranging from slender anguilliform to

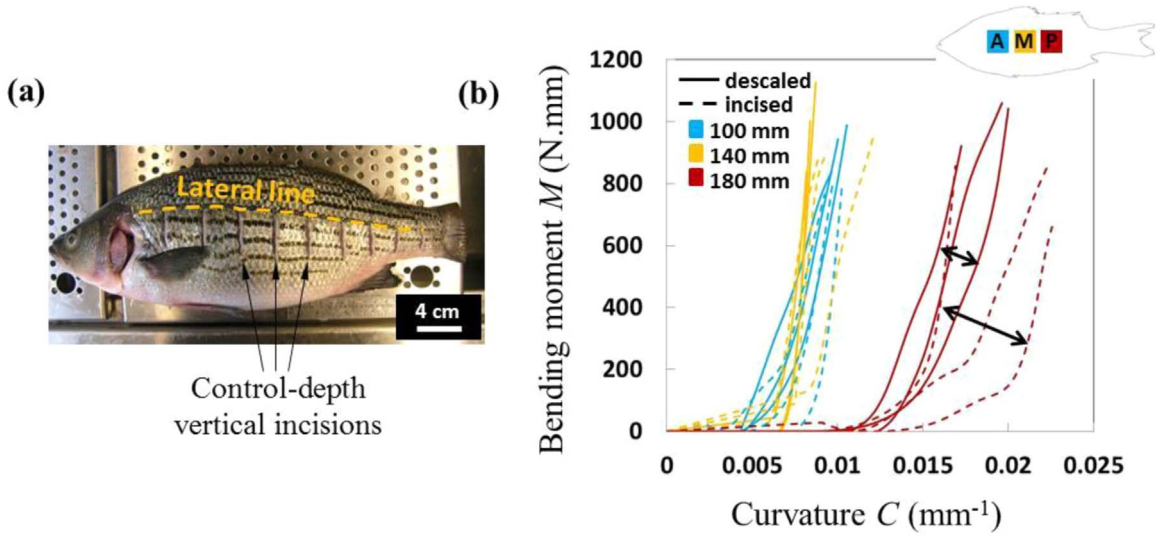

Fig. 7. (a) Fish sample used in bending tests showing control-depth incisions made to the s. compactum. (b) Bending moment versus curvature at three locations along the mid-dorsal line: 100 mm in the anterior region, 140 mm in the mid-region and 180 mm in the posterior region, for a striped bass fish in both "descaled" and s. compactum "incised" conditions (black arrows indicate the rightward shift of *M-C* curves at 180 mm after s. compactum incision).

thicker carangiform (fusiform) body type. The effect of body size on flexural stiffness is not only seen across species of differing body types, but also along an individual fish of a certain species if cross-sectional area (*XSA*) varies along the fish. The most evident variable that changes with anteroposterior body position for striped bass that could affect local flexural stiffness is thickness of the body itself or body *XSA*, which seems to be a reasonable explanation for the markedly higher stiffness values recorded for the thick mid-portion of the striped bass fish. *XSA* and second moment of area with respect to the *y* axis (I_y) (dorsoventral axis) increase markedly along the anteroposterior axis of a typical striped bass specimen from either end of the fish to the middle trunk region (peak *XSA* and I_y were ~6 cm^2 and ~4 × 10^6 mm^4, respectively, at a curvilinear length of ~150 mm). The 3D surface plot of *M-C* along the length of striped bass differs from expected results for an object of cylindrical shape (nearer to the gar fish body type), which should exhibit uniform flexural stiffness along the length of the cylinder.

Long et al. (1996) not only performed bending tests on longnose gar in the scaled condition (skin intact), but also after dermal incisions followed by partial descaling of the fish (removal of a scale row). A rightward shift of the *M-C* curve was observed after these ablation treatments and significant decrease in flexural stiffness (measured 10 m^{-1} past the end of the "neutral zone") of the fish was determined. An insignificant decrease in flexural stiffness was observed after partial descaling of the fish. These results demonstrate an effect of dermal incision and suggest a possible small effect of descaling on the flexural stiffness of the gar fish. The main objective of this study was to reveal a possible substantial decrease in stiffness or slope of the *M-C* curve upon descaling of the fish and not to determine precise mechanical properties of the fish in the natural or descaled condition, and these data demonstrated a lack of a major effect of descaling on the flexural response of the whole fish. This is not surprising given the thicker and more heavily mineralized ganoid scales of the gar fish and its slender body. The effect of descaling on flexural stiffness of striped bass is negligible or undetectable using this experimental setup, and suggests that interlocking of scales during undulatory locomotion does not serve an important mechanical role by acting as a whole body exotendon and facilitating muscle contraction during swimming.

Recent experiments on striped bass employing probe tests of the body surface and digital image correlation revealed the mechanical interaction of fish scales and their local effects on puncture resistance (Zhu et al., 2013). However, this work demonstrates that the mechanical interaction of scales at high body curvatures during swimming has minimal effects on flexural stiffness and thus swimming mechanics, which, similar to the decreased size and weight of teleost scales compared to primitive scale types, may be an adaptation for improved speed, flexibility and maneuverability of teleost fish (Zhu et al., 2012). These results for striped bass are the first to reveal a lack of an exotendon effect provided specifically by the scales during locomotion. Whereas previous authors have also suggested the absence of an external tendon effect for the intact skin (including scales and underlying dermis) of other teleosts (Hebrank and Hebrank, 1986), it has recently been investigated using the methods developed here and with additional histology and mechanical testing whether or not the subjacent dermal tissue (s. compactum) in striped bass functions in the locomotion of this teleost fish via an exotendon effect (Szewciw and Barthelat, 2017). As suggested from the flexural tests after s. compactum incision and further explored in Szewciw and Barthelat (2017), the lack of an external tendon effect during locomotion provided by the scales on the compressed, concave side of the bent fish may be compensated for by the proposed exotendon effect of the underlying s. compactum layer of skin on the stretched, convex side of the bent fish (Elliot, 2000; Wainwright et al., 1978; Hebrank and Hebrank, 1986; Naresh et al., 1997; Szewciw and Barthelat, 2017; Whitear, 1986). This effect is confirmed by the flexural experiments on fish with disrupted s. compactum that we presented here. Data from this research on the contribution of scales and skin to the mechanics of teleost locomotion, in conjunction with previous knowledge on the puncture mechanics of teleost fish skin (Zhu et al., 2012, 2013), can be used in the design and production of synthetic, flexible, protective and locomotory systems for biomimetic applications.

Acknowledgements

This project was supported by the National Science Foundation [CMMI0927585 to F.B.]; and by a Natural Sciences and Engineering Research Council (NSERC) Discovery grant to F.B. L.S. was partially supported by a McGill Engineering Doctoral Award from the Faculty of Engineering at McGill University.

References

Aleyev, Y.G., 1977. Nekton. W. Junk, The Hague.
Browning, A., Ortiz, C., Boyce, M.C., 2013. Mechanics of composite elasmoid fish scale assemblies and their bioinspired analogues. J. Mech. Behav. Biomed. Mater. 19, 75–86.
Bruet, B.J.F., Song, J.H., Boyce, M.C., Ortiz, C., 2008. Materials design principles of ancient fish armour. Nat. Mater. 7, 748–756.
Chintapalli, R., Mirkhalaf, M., Dastjerdi, A.K., Barthelat, F., 2014. Fabrication, testing and modeling of a new flexible armor inspired from natural fish scales and osteoderms. Bioinspir. Biomim. 9, 036005.
De luliis, G., Pulera, D., 2001. The Dissection of Vertebrates: A Laboratory Manual, second ed. Academic Press, Burlington.
Elliot, D.G., 2000. Chapter 5 - Integumentary system (Gross Functional Anatomy), Chapter 17 - Integumentary system (Microscopic Functional Anatomy). In: Ostrander, G.K. (Ed.), The Laboratory Fish 271–306. Academic Press, Oxford, pp. 95–108.
Garrano, A.M.C., La Rosa, G., Zhang, D., Niu, L.-N., Tay, F.R., Majd, H., Arola, D., 2012. On the mechanical behavior of scales from *Cyprinus carpio*. J. Mech. Behav. Biomed. Mater. 7, 17–29.
Ghosh, R., Ebrahimi, H., Vaziri, A., 2014. Contact kinematics of biomimetic scales. Appl. Phys. Lett. 105, 233701.
Hebrank, M.R., Hebrank, J.H., 1986. The mechanics of fish skin: lack of an "external tendon" role in two teleosts. Biol. Bull. 171, 236–247.
Hodson, R.G., 1989. Hybrid striped bass: biology and life history. SRAC 300, 1–4.
Huss, H.H., 1995. Quality and quality changes in fresh fish. FAO Fisheries Technical Paper 348. ISBN 92-5-103507-5.
Ikoma, T., Kobayashi, H., Tanaka, J., Walsh, D., Mann, S., 2003. Microstructure, mechanical, and biomimetic properties of fish scales from *Pagrus major*. J. Struct. Biol. 142, 327–333.
Jayne, B.C., Lauder, G.V., 1995. Speed effects on midline kinematics during steady undulatory swimming of largemouth bass, *Micropterus salmoides*. J. Exp. Biol. 198, 585–602.
Long, J.H., Hale, M.E., McHenry, M.J., Westneat, M.W., 1996. Functions of fish skin: flexural stiffness and steady swimming of longnose gar, *Lepisosteus osseus*. J. Exp. Biol. 199, 2139–2151.
Matlab version R2011b, ⟨http://www.mathworks.com/⟩.
Martini, R., Barthelat, F., 2016a. Stretch-and-release fabrication, testing and optimization of a flexible ceramic armor inspired from fish scales. Bioinspir. Biomim. 11, 066001.
Martini, R., Barthelat, F., 2016b. Stability of hard plates on soft substrates and application to the design of bioinspired segmented armor. J. Mech. Phys. Solids 92, 195–209.
Martini, R., Balit, Y., Barthelat, F., 2017. A comparative study of bio-inspired protective scales using 3D printing and mechanical testing. Acta Biomater [to appear].
Meyers, M.A., Lin, Y.S., Olevsky, E.A., Chen, P.-Y., 2012. Battle in the Amazon: arapaima versus Piranha. Adv. Eng. Mater. 14, B279–B288.
Naresh, M.D., Arumugam, V., Sanjeevi, R., 1997. Mechanical behaviour of shark skin. J. Biosci. 22, 431–437.
Plot Digitizer version 1.9, ⟨http://plotdigitizer.sourceforge.net/⟩.
Rudykh, S., Ortiz, C., Boyce, M.C., 2015. Flexibility and protection by design: imbricated hybrid microstructures of bio-inspired armor. Soft Matter 11, 2547–2554.
Szewciw, L., Barthelat, F., 2017. Mechanical properties of striped bass fish skin: Evidence of an exotendon function of the stratum compactum. J. Mech. Behav. Biomed. Mater. (to appear).
Torres, F.G., Troncoso, O.P., Nakamatsu, J., Grande, C.J., Gomez, C.M., 2008. Characterization of the nanocomposite laminate structure occurring in fish scales from *Arapaima gigas*. Mater. Sci. Eng. C 28, 1276–1283.
Tytell, E.D., Borazjani, I., Sotiropoulos, F., Baker, T.V., Anderson, E.J., Lauder, G.V., 2010. Disentangling the functional roles of morphology and motion in the swimming of fish. Int. Comp. Biol. 50, 1140–1154.
Vernerey, F.J., Barthelat, F., 2010. On the mechanics of fishscale structures. Int. J. Solids Struct. 47, 2268–2275.
Wainwright, S.A., Vosburgh, F., Hebrank, J.H., 1978. Shark skin: function in locomotion. Science 202, 747–749.
Whitear, M., 1986. The skin of fishes including cyclostomes. In: Bereiter-Hahn, J., Matoltsy, A., Richards, K. (Eds.), Biology of the Integument – 2 Vertebrates. Springer-Verlag, Berlin, pp. 8–77.
Yang, W., Chen, I.H., Gludovatz, B., Zimmermann, E.A., Ritchie, R.O., Meyers, M.A., 2013. Natural flexible dermal armor. Adv. Mater. 25, 31–48.
Zhu, D., Fuentes-Ortega, C., Motamedi, R., Szewciw, L., Vernerey, F., Barthelat, F., 2012. Structure and mechanical performance of a "modern" fish scale. Adv. Eng. Mater. 14, B185–B194.
Zhu, D., Szewciw, L., Vernerey, F., Barthelat, F., 2013. Puncture resistance of the scaled skin from striped bass: collective mechanisms and inspiration for new flexible armor designs. J. Mech. Behav. Biomed. Mater. 24, 30–40.